Acta Crystallographica Section A
Foundations of Crystallography
ISSN 0108-7673

Received 14 November 2001
Accepted 16 January 2002

Local squaring functions

Jeffrey Roach and Charles W. Carter Jr*

Department of Biochemistry and Biophysics, University of North Carolina, Chapel Hill, NC 27599, USA. Correspondence e-mail: carter@med.unc.edu

Simple modifications to the Sayre squaring method determine a class of functional atomic form constraints representing the likelihood that a particular atomic form occupies a localized volume of the unit cell. The functional formulation, as opposed to the traditional structure-factor equation formulation, facilitates modeling multiple atom types and integrating atomic form information into established density-modification routines. Two complementary methods of phase refinement are considered. The first method constructs an atomic resolution probabilistic filter from the atomic form functions. The probabilistic filter is used to modify density throughout the unit cell, in both the solvent and macromolecular regions of the unit cell. The second method exploits the automated map interpretation aspects of the atomic form functions. A simple iterative phase-refinement procedure alternating the two methods successively is applied to three small metalloproteins, with significant phase improvements beyond that obtained with conventional density modification or refinement in accordance with reciprocal-space squaring equations.

1. Introduction

It is widely recognized that, in the absence of non-crystallographic symmetry, solvent-flattening techniques (Wang, 1985; Abrahams & Leslie, 1996; Xiang *et al.*, 1993) provide one of the most effective physical constraints on the electron density for use in phase determination for macromolecular structures. Solvent-flattening methods are based on the observation that the unit cell of a macromolecular crystal can be divided into distinct macromolecular and solvent regions. In physical terms, the electron density of the solvent region should be largely diffuse and areas of significant density can be assumed to be in error. Therefore, choosing phases that dampen electron-density fluctuations in the solvent region as much as possible leads to a better phase set.

Solvent-flattening techniques, however, can only modify density in the solvent region to determine and refine phases. To make more effective use of density constraints throughout the entire unit cell, solvent-flattening techniques have been generalized to analyze the shape of the frequency histogram produced by the electron density (Zhang & Main, 1990; Terwilliger, 2000). So-called 'histogram-matching' methods (Lunin, 1993; Zhang, 1993) constrain the density histogram to deviate minimally from an ideal density histogram. The electron-density histogram does not, however, represent fully all of the structural information present in the macromolecular region of the unit cell. Additional information can be captured by multi-dimensional histogram-matching methods which assess local quantities of the electron density, such as local mean, local variance, gradient and Laplacian (Xiang & Carter, 1996; Nieh & Zhang, 1999; Refaat *et al.*, 1996). These multi-dimensional histograms encode valuable structural information; however, it is available only indirectly.

Direct structural information is available, given atomic resolution, from the atomic forms. Atomic form constraints, such as the Sayre *squaring method equations* (Sayre, 1952), and generalizations thereof due to Woolfson (1958), Von Eller (1973) and Rothbauer (2000), were among the first methods exploited in the structure determination of small molecules. These constraints traditionally take the form of convolutional structure-factor equations for which a least-squares solution can in principle be determined. Consider, as an example, the Sayre squaring method equations for each reflection h:

$$a_h F_h = \sum_k F_k F_{h-k},$$

where a_h is determined from the single modeled atom form. The least-squares solution, in this case, corresponds to a set of phases for which the quantity

$$D = \sum_h \left| a_h F_h - \sum_k F_k F_{h-k} \right|^2$$

is minimized (Sayre, 1972, 1974; Debaerdemaeker *et al.*, 1988; Refaat *et al.*, 1995). By Parseval's theorem, the quantity being minimized, D, is equal to an integral over the entire unit cell. Since the atom-form constraints are true only approximately, some parts of the unit cell are more accurately reflected in the structure-factor constraints than others and the mean deviation throughout the unit cell is not necessarily meaningful. Consequently, minimizing what is, in effect, an average value throughout the unit cell is not extremely effective. In fact, it

has been shown that the correct structure need not have the lowest D value among all possible structures (Roach *et al.*, 2001). Furthermore, the convolutional nature of the constraints hinders any attempt to determine meaningful weights constraining the contribution to D of individual phases. Nonetheless, the atomic form constraints do possess valuable structure-determining information; unfortunately, this information is presented in a form that makes it difficult to access through least-squares refinement. We show here that in order to exploit atomic shape information more efficiently for phase refinement, the atomic form constraints must take a somewhat different formulation.

Functions are developed that express the likelihood that a localized volume of the unit cell corresponds to an atom of a prescribed form. Owing to the localization, these likelihood functions are not subject to an equal-atom condition, but can correspond to each different atom type known to occur in the structure. Taken together, they determine an atomic resolution probabilistic filter of the structure. This probabilistic filter forms the basis of an iterative phase-refinement algorithm combining both solvent and model-independent macromolecular density-modification methods with iterative model building.

2. Local squaring functions

For a given atomic form ϱ_0, consider the function $f(x)$ determined by the product of the electron density ϱ and this atomic form centered at y within the unit cell:

$$f(x) = \varrho(x)\varrho_0(x - y).$$

If the electron density contains an atom of type ϱ_0 located at y, the function f will approximate the squared atomic form centered on the point y:

$$\varrho_0^2(x - y);$$

otherwise f will take some other form. Note that the quality of this approximation will depend on both the resolution of the map and, importantly, on the error in the phases used to construct it. Assuming sufficient resolution, the likelihood that a given point in the unit cell is the center of an atom of type ϱ_0 will be measured by the similarity between f and the squared atom form. To express similarity in terms of the least-squares difference between these functions, the local squaring function is defined as

$$O(y) = \int_V |\varrho(x)\varrho_0(x - y) - \varrho_0^2(x - y)|^2 \, \mathrm{d}x^3. \qquad (1)$$

Note that $O(y)$ will be close to zero at points of the unit cell that are most likely to be the centers of atoms of the form ϱ_0.

For simplicity, assume that ϱ takes only real values and that ϱ_0 is centrosymmetric. The structure factors of this function, O_h, are easily determined from the expansion

$$O(y) = \int_V [\varrho^2(x)\varrho_0^2(x - y) - 2\varrho(x)\varrho_0^3(x - y) + \varrho_0^4(x - y)] \, \mathrm{d}x^3.$$

Thus, letting $f_h^{(n)}$ denote the scattering factor of the atom form ϱ_0^n and $|V|$ denote the volume of the unit cell,

$$O_h = [f_h^{(2)}/|V|] \sum_k F_k F_{h-k} - 2F_h f_h^{(3)} + \delta(h) \int_V \varrho_0^4(x) \, \mathrm{d}x^3,$$

where δ is the Kronecker delta, taking the value 1 for $h = 0$ and 0 otherwise. Therefore, the local squaring functions for a particular atom type can be calculated efficiently by reducing the convolution to fast Fourier transforms.

3. Phase refinement

Electron-density maps constructed from experimentally determined phases are seldom optimal for interpretation and model building. The quality of the structural information to be obtained depends on the degree to which the experimental phases can be adjusted to improve the electron-density map they determine. Typically, the phases are adjusted in order to satisfy more closely some general principle, such as the distinction between macromolecule and solvent regions of the unit cell. We consider two complementary methods, A and B, of utilizing the atomic form information inherent in the local squaring functions for phase refinement.

Method A is closely related to solvent flattening. Solvent-flattening techniques determine phases that minimize density fluctuation in the solvent region. The local squaring functions have the property of taking values close to zero in the regions of the unit cell that are likely to contain an atom of a particular form. Thus they provide an objective function analogous to solvent flatness for the electron density within the molecular envelope. Therefore, combining several properly scaled local squaring functions corresponding to different atom types will produce an atomic resolution probability map that can improve density within the molecular envelope.

Given a set of suitable atomic forms, $\{\varrho_i\}$, $1 \leq i \leq N$, consider the local squaring functions defined by each atomic form: $\{O_i\}$, $1 \leq i \leq N$. Define a probability function on the unit cell as follows:

$$P_i(x) = \exp\{-\alpha_i[O_i(x) + \beta_i]\}, \qquad x \in V,$$

where α_i and β_i are constants, specific to each atom type, normalizing the scale of the local squaring function. Note that β_i are necessary to ensure that $P_i(x)$ is greater than or equal to zero and less than or equal to one. Theoretically, this is guaranteed by (1); however, in practice finite resolution will cause these functions to take some negative values. Once the probability functions have been determined, they can be combined recursively into a single probability function expressing the probability that an atom of any of the given forms occupies a particular volume within the unit cell.

Let $P_i'(x)$ denote the probability determined by the local squaring functions corresponding to the first i atom types. That is, the probability that a particular region corresponds to an atom of the first type or an atom of the second type, and so forth. Thus,

$$P_1'(x) = P_1(x)$$

and each additional atom type is introduced recursively as

$$P_{i+1}' = P_i'(x) + P_{i+1}(x) - P_i'(x)P_{i+1}(x).$$

Note that the product is necessary because the probabilities corresponding to different atom types are not necessarily disjoint. We do, however, assume that they are independent. The resulting function, $P'_N(x)$, or more simply $P(x)$, combines the information from the local squaring functions for different atom types into an atomic resolution probabilistic filter.

Consider next the product $\varrho(x)P(x)$. Since $P(x)$ takes values near 1 in regions that are likely to contain atoms of a particular form, these regions are mostly preserved in $\varrho(x)P(x)$. However, in regions where $P(x)$ takes values near 0, *i.e.* regions unlikely to contain atoms of the prescribed form, the density of $\varrho(x)P(x)$ will be dampened. This observation is the basis for the method *A* phase-refinement scheme.

Let $\varrho^{(n)}$ and $P^{(n)}$ denote the electron-density map and probability map obtained after n iterations, respectively. A new set of phases is determined from the average of the current map $\varrho^{(n)}$ and the product $P^{(n)}\varrho^{(n)}$, *i.e.*

$$\varrho^{(n+1)} = [\varrho^{(n)} + P^{(n)}\varrho^{(n)}]/2.$$

The probabilistic filter can also benefit from the iterative construction. For example,

$$P^{(n)}(x) = P(x) + \zeta(x)P^{(n-1)}(x),$$

where $\zeta(x)$ introduces information from previous steps and, potentially, other independent sources. In particular, traditional density-modification methods or map quality estimates from experimental sources could be included.

The current implementation of method *A* determines the scaling constants α and β from the initial data and the value of ζ remains constant throughout the calculation. The fast Fourier transform routines are taken from the *Digital Extended Math Library for Digital UNIX Signal Processing* subcomponent (Digital Equipment Corporation, 1999). A sampling grid that is approximately twice as fine as the Shannon–Nyquist requirement is used.

The local squaring functions represent an implicit interpretation of the electron density in terms of atoms of a particular type and their likely coordinates. Method *B* exploits these map-interpretation properties. For a given atomic form, the negative of the local squaring function will have distinct peaks corresponding to the locations of atoms of the given form. Therefore, a list of atomic locations for each atomic form is generated by examining the corresponding local squaring function. This list of atomic coordinates is then used to construct a new electron density, $\hat{\varrho}_1$. A second application of this method applied to $\varrho - \hat{\varrho}_1$ will often lead to additional atomic peaks that were not present in $\hat{\varrho}_1$. Let the electron density generated by the second set of peaks be denoted $\hat{\varrho}_2$. The list of peaks determined by both passes of the method can be used for model specification or used in an iterative averaging scheme. Let $\hat{\varrho}$ denote the electron density determined by both sets of peaks, then

$$\varrho^{(n+1)} = [\varrho^{(n)} + \hat{\varrho}]/2$$

determines the map from which a new set of phases is derived.

The current implementation of method *B* makes use of the routine *peakmax* taken from the *CCP4* suite (Collaborative Computational Project, Number 4, 1994). The input map for this routine is sampled on a grid that is approximately five times the Shannon–Nyquist requirement.

We envision that the appropriate use of these methods will be in the context of components in larger more established structure-determination systems. The important advantage that the local squaring functions provide over traditional structure-factor equations and conventional density modification is the ability to model multiple different atomic forms within the molecular envelope in a formulation resembling common density-modification techniques, such as solvent flattening. This formulation allows atomic form constraints to make more substantial contributions to systems consisting of multiple constraints. For example, in *ACORN* (Foadi *et al.*, 2000), where atomic form information is evaluated in the context of Sayre's equations, the local squaring functions could provide a more effective complement to dynamic density modification. Furthermore, the probabilistic filter derived from the local squaring functions represents an implicit natural foundation for automated map interpretation. In a system such as *wARP* (Perrakis *et al.*, 1997), where a probable atomic model is constructed in increments, the probabilistic filter provides an alternative to coordinate refinement and an excellent basis for introducing new elements of the model.

4. Examples

To demonstrate the effectiveness of methods *A* and *B* in this communication, consider an algorithm, resembling *Shake-and-Bake* (Weeks *et al.*, 1994) or *SHELXD* (Sheldrick & Gould, 1995), where methods *A* and *B* are applied successively. We applied this algorithm to three small metalloproteins: wild-type rubredoxin, Zn-substituted rubredoxin and high-potential iron protein. In each of the rubredoxin examples, local squaring functions corresponding to three atom types are used: an average C, N, O type; an S type; and a metal type (Fe or Zn). For the high-potential iron protein, a fourth atom type corresponding to solvent O proved beneficial.

4.1. Wild-type rubredoxin

Rubredoxin is a small non-heme iron protein, the structure of which has been studied in great detail. Intensities and experimentally derived phases for this particular specimen were measured by Dauter *et al.* (1996) to 1.1 Å. The experimental phases were then processed by *dm* (Cowtan, 1994) and used to construct an initial set of structure factors to 1.2 Å.

The results of applying method *A* and method *B* successively are given in Table 1. Note that although a second application of method *B* can indeed lead to a slight improvement in the map correlation coefficient, the mean phase error in all resolution bands does not improve. Nonetheless, we obtain an overall improvement of more than 23° in mean phase error with an improvement of more than 30° for the highest resolution band, and nearly 0.2 in map correlation

Table 1
Phase error and map correlation with respect to wild-type rubredoxin coordinates.

The mean phase error for each resolution ring is given in degrees for each sequence of methods.

Resolution	Initial	*A*	*AB*	*ABA*	*ABAB*	*ABABA*
>2.0 Å	49.342	49.385	49.153	41.901	41.994	41.510
2.0–1.8 Å	54.134	53.006	52.231	36.628	37.868	36.436
1.8–1.6 Å	57.941	53.505	52.331	35.109	36.266	34.216
1.6–1.4 Å	65.532	56.959	56.282	37.829	38.357	36.723
1.4–1.2 Å	70.677	58.587	57.915	40.828	40.868	39.630
>1.2 Å	62.044	55.164	54.515	39.377	39.767	38.493
Map *R*	0.584	0.648	0.665	0.770	0.774	0.777

Table 2
Phase error and map correlation with respect to zinc rubredoxin coordinates.

The mean phase error for each resolution ring is given in degrees for each sequence of methods

Resolution	Initial	*A*	*AB*	*ABA*	*ABAB*	*ABABA*
>2.0 Å	42.873	40.038	37.138	31.573	32.227	31.479
2.0–1.8 Å	49.489	44.268	40.105	26.195	28.290	26.221
1.8–1.6 Å	56.520	46.814	40.990	24.459	26.774	24.489
1.6–1.4 Å	64.244	51.843	46.153	28.173	29.688	27.757
1.4–1.2 Å	70.767	59.185	54.579	33.600	33.879	32.612
>1.2 Å	59.893	50.615	46.034	30.229	31.261	29.772
Map *R*	0.676	0.782	0.813	0.873	0.874	0.876

coefficient. Fig. 1 gives a representative sample of the refined electron-density map.

4.2. Zn-substituted rubredoxin

The wild-type rubredoxin active site consists of a single Fe atom coordinated tetragonally to four cysteinyl S atoms. This binding motif is similar to the metal core found in the Zn-finger family. In order to study this ZnS_4 unit, Dauter *et al.* (1996) constructed as a structural model a Zn-substituted rubredoxin. A set of structure factors for this protein at 1.2 Å resolution were again derived from *dm*-processed experimental phases.

The initial phase set for the Zn-substituted rubredoxin is significantly better than that of the wild type. The better initial phases lead to an improvement of nearly 40° in the mean phase error of the highest-resolution band, an improvement in overall mean phase error of more than 30° and an improvement of map correlation by 0.2. The mean phase error for each resolution band and map correlation coefficients are given in Table 2. Fig. 2 shows the refined electron density around the metal cluster.

4.3. High-potential iron protein

Another Fe–S cluster of considerable biological interest is $[Fe_4S_4]$. Carter *et al.* (1972) determined the intricate interpenetrating tetrahedral structure of this cluster in the high-potential iron protein at 2.0 Å resolution. The 0.93 Å structure of an H42Q mutant of this protein has been shown by Parisini *et al.* (1999) to be essentially isostructural. To test the local-squaring-function-based methods on phases exhibiting some model bias, the following system of structure factors was constructed. A 2.0 Å phase set was calculated from the wild-type oxidized structure by superimposing its four Fe atoms on the four Fe atoms of the mutant. Sharpening the structure factors obtained from these phases and the experimental intensities for the mutant deposited in the Protein Data Bank, we generated a 1.0 Å set of structure factors by the phase-extrapolation procedure discussed by Roach *et al.* (2001).

This example differs from the previous two in that the errors in the initial phase set are systematic as opposed to random. For the purpose of comparison, we consider a map

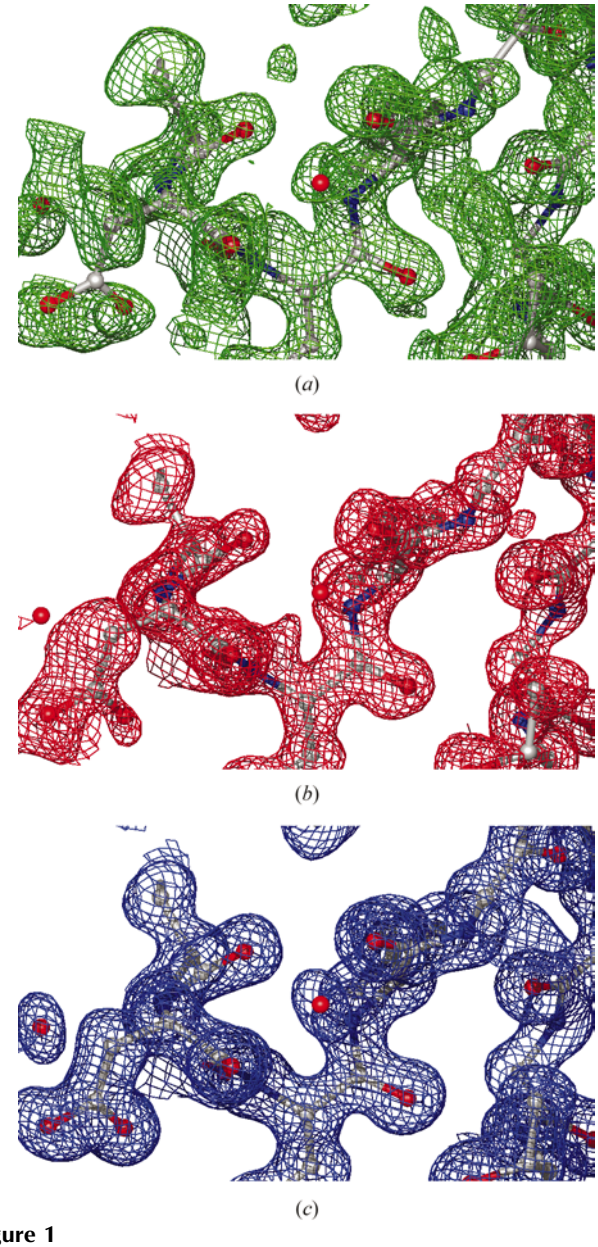

Figure 1
Representative electron-density maps for wild-type rubredoxin. Each map is contoured at 1.2 standard deviations from its mean. (*a*) The initial electron density. (*b*) The refined map. (*c*) The model-calculated electron density.

Table 3
Phase error and map correlation with respect to H42Q mutant high-potential iron protein coordinates.

The mean phase error for each resolution ring is given in degrees for each sequence of methods. The phase set denoted 'Compare' consists of phases calculated from the wild-type model to 10 Å.

Resolution	Initial	*A*	*AB*	*ABA*	Compare
>2.0 Å	48.131	40.776	40.933	40.465	48.131
2.0–1.75 Å	60.472	34.306	33.134	33.207	53.615
1.75–1.5 Å	47.747	33.899	33.143	33.048	54.757
1.5–1.25 Å	50.095	32.619	32.232	31.604	61.519
1.25–1.0 Å	49.705	32.332	29.743	29.787	64.764
>1.0 Å	49.929	33.875	32.438	32.253	60.087
Map *R*	0.741	0.831	0.839	0.837	0.729

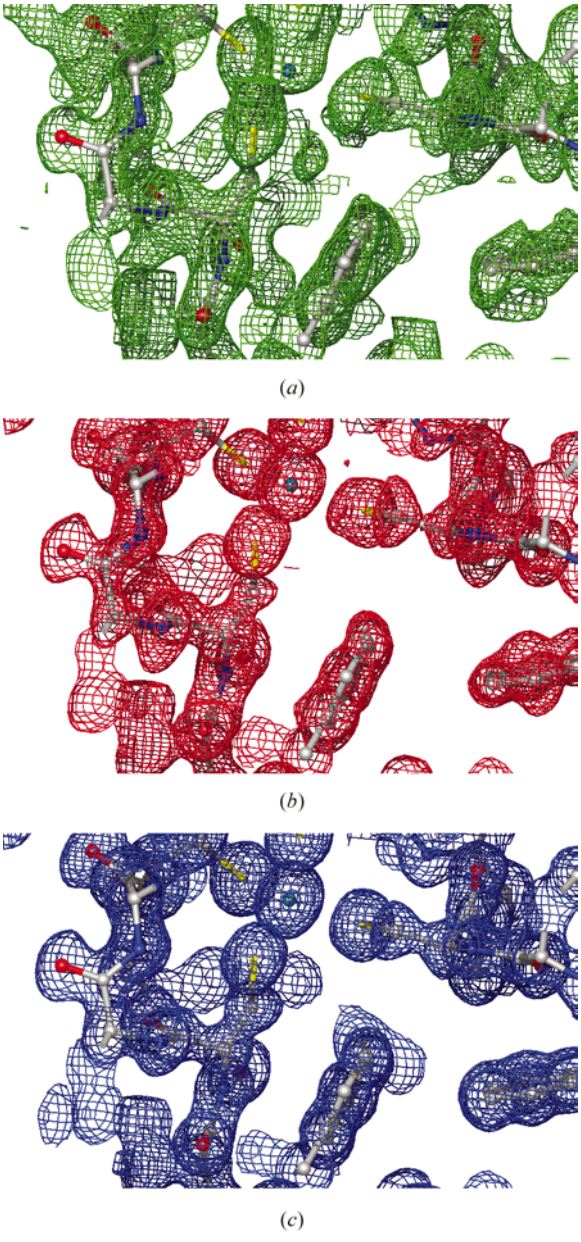

Figure 2
Electron density surrounding the metal cluster of Zn-substituted rubredoxin. Each map is contoured at 1.2 standard deviations from its mean. (*a*) The initial electron density. (*b*) The refined map. (*c*) The model-calculated electron density.

constructed from the experimental amplitudes with phases calculated from the lower resolution model. The mean phase error and map correlation coefficients are given in Table 3. Note particularly that the phase errors have improved by more than 15° from the initial extrapolated phases. In the highest resolution band, the mean phase error is nearly 30° better than those based on the wild-type model. Fig. 3 displays the electron density around the mutation. Although the glutamine 42 side-chain density in the refined map is incomplete for the N_γ, the entire, incorrect, wild-type histidine residue structure is intact in the comparison map.

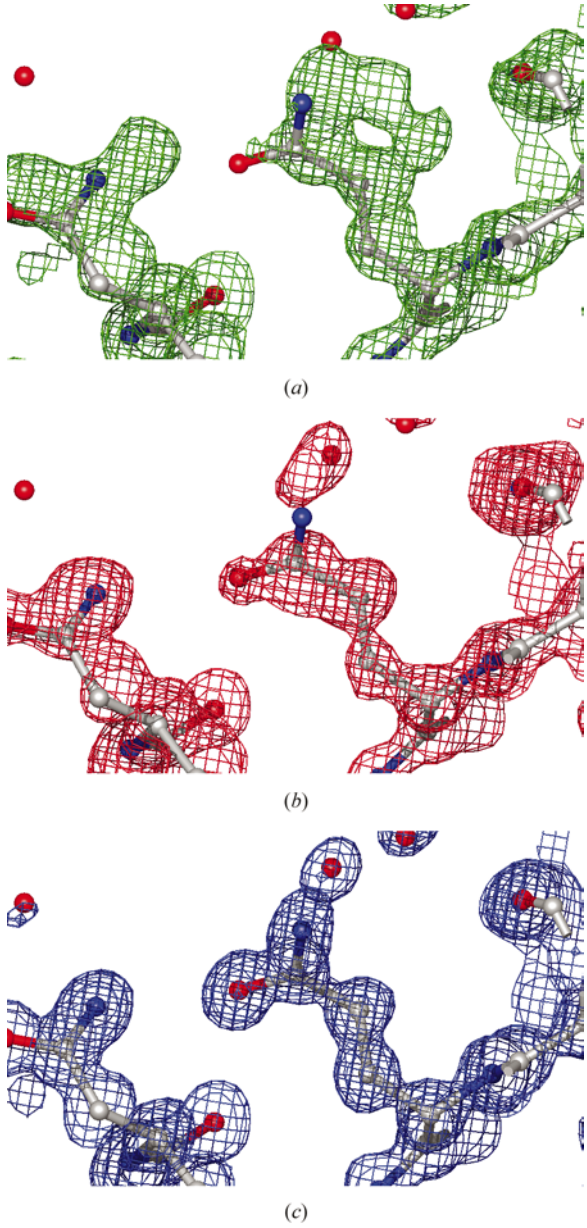

Figure 3
Electron density corresponding to H42Q mutation in high-potential iron protein. Each map is contoured at 1.2 standard deviations from its mean. (*a*) The electron density constructed from experimental amplitudes and phases of wild type. (*b*) The refined electron-density map. (*c*) The coordinate-refined electron density.

5. Conclusions

Although the development of the local squaring functions is still in its infancy, a number of promising aspects of the functions have been illustrated. Notably, the local squaring functions encapsulate atomic form constraints in a form suitable for phase refinement, either alone or in conjunction with more established methods. In particular, the local squaring functions appear to be high-resolution complements to methods such as solvent flattening and histogram matching, which are more effective at lower resolution. The examples in Tables 1, 2 and 3 suggest that mean phase-error improvements of up to 40° beyond that achieved with *dm* are possible for high-resolution reflections. Also notable, in view of our previous inability to refine low-resolution phases using the convolutional structure-factor equations of Sayre and Woolfson (Roach *et al.*, 2001), is that the phases to 2.0 Å improved by around 10° in each of the three examples. Moreover, the phase-refinement methods derived from the local squaring functions incorporate multiple atom types more easily than the methods of Woolfson (1958), Von Eller (1973) and Rothbauer (2000).

Local squaring function phase refinement remains far from optimized. Certain methodological improvements are immediately suggested. For example, in method *A*, allowing the function *P* to take negative values would in effect simulate a solvent flipping technique (Abrahams & Leslie, 1996); method *B* could be adapted to place entire subunits, such as amino acids rather than simply single atoms; and both methods would benefit by replacing the simple averaging scheme with a more sophisticated procedure exploiting Sim weights (Sim, 1960) to represent estimated phase errors. Other questions, particularly involving scaling and resolution dependence, await satisfactory investigation. Nevertheless, the promise embodied in the preliminary results suggests that such investigations would be worthwhile.

As the phase-refinement aspects of the local squaring functions have been only touched upon, other properties, such as the map interpretation aspects, remain completely unexplored. Method *B* exploited these properties for the purpose of phase refinement; however, more far-reaching applications are not unreasonable. In particular, there is an emerging realization that phase determination, model building and coordinate refinement are, and ought to be considered to be, more closely linked than was previously recognized (Lamzin *et al.*, 2000). It would be extremely interesting to develop statistical foundations sufficient to support local-squaring-function-based hypothesis testing applied to automated model construction.

We would like to thank Z. Dauter for providing experimental intensities and phases for both rubredoxin proteins studied in this communication.

References

Abrahams, J. P. & Leslie, A. (1996). *Acta Cryst.* D**52**, 30–42.
Carter, C. W. Jr, Kraut, J., Freer, S. T., Alden, R. A., Sieker, L. C., Adman, E. & Jensen, L. H. (1972). *Proc. Natl Acad. Sci. USA*, **69**, 3526–3529.
Collaborative Computational Project, Number 4 (1994). *Acta Cryst.* D**50**, 760–763.
Cowtan, K. D. (1994). *Joint CCP4/ESF-EACBM Newslett. Protein Crystallogr.* **31**, 34–38.
Dauter, Z., Wilson, K. S., Sieker, L. C., Moulis, J.-M. & Meyer, J. (1996). *Proc. Natl Acad. Sci. USA*, **93**, 8836–8840.
Debaerdemaeker, T., Tate, C. & Woolfson, M. M. (1988). *Acta Cryst.* A**44**, 353–357.
Digital Equipment Corporation (1999). *Digital Extended Math Library for Digital UNIX Reference Manual*. Maynard, MA, USA.
Foadi, J., Woolfson, M. M., Dodson, E. J., Wilson, K. S., Yao, J.-X. & Zheng, C.-D. (2000). *Acta Cryst.* D**56**, 1137–1147.
Lamzin, V. S., Perrakis, A., Bricogne, G., Jiang, J., Swaminathan, S. & Sussman, J. L. (2000). *Acta Cryst.* D**56**, 1510–1511.
Lunin, V. Yu. (1993). *Acta Cryst.* D**49**, 90–99.
Nieh, Y.-P. & Zhang, K. Y. J. (1999). *Acta Cryst.* D**55**, 1893–1900.
Parisini, E., Capozzi, F., Lubini, P., Lamzin, V., Luchinat, C. & Sheldrick, G. M. (1999). *Acta Cryst.* D**55**, 1773–1784.
Perrakis, A., Sixma, T. K., Wilson, K. S. & Lamzin, V. S. (1997). *Acta Cryst.* D**53**, 448–455.
Refaat, L. S., Tate, C. & Woolfson, M. M. (1995). *Acta Cryst.* D**51**, 1036–1040.
Refaat, L. S., Tate, C. & Woolfson, M. M. (1996). *Acta Cryst.* D**52**, 252–256.
Roach, J., Retailleau, P. & Carter, C. W. Jr (2001). *Acta Cryst.* A**57**, 341–350.
Rothbauer, R. (2000). *Z. Kristallogr.* **215**, 157–168.
Sayre, D. (1952). *Acta Cryst.* **5**, 60–65.
Sayre, D. (1972). *Acta Cryst.* A**28**, 210–212.
Sayre, D. (1974). *Acta Cryst.* A**30**, 180–184.
Sheldrick, G. M. & Gould, R. O. (1995). *Acta Cryst.* B**51**, 423–431.
Sim, G. A. (1960). *Acta Cryst.* **13**, 511–512.
Terwilliger, T. C. (2000). *Acta Cryst.* D**56**, 965–972.
Von Eller, G. (1973). *Acta Cryst.* A**29**, 63–67.
Wang, B.-C. (1985). *Methods Enzymol.* **115**, 90–112.
Weeks, C. M., DeTitta, G. T., Hauptman, H. A., Thurman, P. & Miller, R. (1994). *Acta Cryst.* A**50**, 210–220.
Woolfson, M. (1958). *Acta Cryst.* **11**, 277–283.
Xiang, S. & Carter, C. W. Jr (1996). *Acta Cryst.* D**52**, 49–56.
Xiang, S., Carter, C. W. Jr, Bricogne, G. & Gilmore, C. J. (1993). *Acta Cryst.* D**49**, 193–212.
Zhang, K. Y. J. (1993). *Acta Cryst.* D**49**, 213–222.
Zhang, K. Y. J. & Main, P. (1990). *Acta Cryst.* A**46**, 377–381.